Coherent tunnelling through two quantum dots with Coulomb interaction

1996 J. Phys.: Condens. Matter 8 5401

(http://iopscience.iop.org/0953-8984/8/29/015)

J. Phys.: Condens. Matter **8** (1996) 5401–5414. Printed in the UK

Coherent tunnelling through two quantum dots with Coulomb interaction

P Pals and A MacKinnon

The Blackett Laboratory, Imperial College, London SW7 2BZ, UK

Received 9 February 1996, in final form 14 May 1996

Abstract. The coherent conductance and current is calculated through two quantum dots using the Hubbard model for a single level per spin. The occurrence of negative differential conductance is demonstrated. The ohmic conductance is calculated for dots with equally spaced levels. Transport is determined by matching energy levels, even when they do not occur at the charge degeneracy points.

1. Introduction

The advance of lithographical techniques on a nanometre scale in recent years has made it possible to study systems that were inaccessible to experimentation before. This has opened the way to produce and investigate structures where the carriers are confined to one or even zero dimensions. This has given rise to the discovery of a number of novel effects. It has been shown by Reed *et al* that discrete states can clearly be discerned in quantum dots, structures which have been confined in all three dimensions [1]. These technological advances have made it possible to study the interplay between charge quantization effects (Coulomb blockade) and size quantization effects (discrete energy levels).

Whereas there has been a considerable amount of experimental and theoretical study on the conductive properties of single quantum dots [2, 3] and single and double metallic dots [4, 5, 6], so far relatively little attention has been paid to the case of two quantum dots in series.

The transport properties of a single dot are insensitive to incoherent scattering, provided that the broadening of the levels is small [7, 8]. However, when two dots are connected in series, this no longer holds true. In this paper the coherent case will be considered where the phase-breaking rate is small compared to the tunnelling rate. Recently, the importance of coherence for transport through a single dots has been shown explicitly by direct measurement of the phase of the transmission coefficient [9].

2. Method

The system under investigation consists of an interacting region of one or more quantum dots connected between leads or electron reservoirs of specified chemical potential. In general the reservoirs will have different chemical potentials, causing a current to flow through the dots. This makes it inherently a non-equilibrium process. Therefore the system will be best described using non-equilibrium Green functions, now commonly referred to as the Keldysh

0953-8984/96/295401+14$19.50

method [10, 11]. This formalism is not only valid in the linear response regime, but also for higher bias voltages. A full description not only requires knowledge of the retarded and advanced Green functions, as in equilibrium, but also of the 'distribution' Green function $G^<$ between the reservoir and dot sites:

$$G^r_{n,m}(t,t') = -\mathrm{i}\Theta(t-t')\langle\{c_n(t), c^\dagger_m(t')\}\rangle \tag{1}$$

$$G^a_{n,m}(t,t') = \mathrm{i}\Theta(t'-t)\langle\{c_n(t), c^\dagger_m(t')\}\rangle \tag{2}$$

$$G^<_{n,m}(t,t') = \mathrm{i}\langle c^\dagger_m(t')c_n(t)\rangle \tag{3}$$

where $c^\dagger$ and c are the usual creation and annihilation operators. In steady state the diagonal elements of $\mathbf{G}^r - \mathbf{G}^a$ are proportional to the local density of states, whereas $\mathbf{G}^<$ plays the role of the density matrix. They are related by the distribution matrix $\mathbf{F}$, defined by $\mathbf{G}^< = -\mathbf{F}(\mathbf{G}^r - \mathbf{G}^a)$. In equilibrium $\mathbf{F}$ is simply a scalar and is identical to the Fermi–Dirac distribution function.

Having introduced the non-equilibrium Green functions, the obvious next step is to find an expression for the Landauer formula [12] relating the current to the local properties of the system, such as the chemical potentials of the reservoirs, the density of states and the average occupation of the dots. It is assumed that the left and right electron reservoirs are large enough to have well-defined Fermi–Dirac distributions, f_L and f_R, and chemical potentials μ_L and μ_R. Any interaction effects in the reservoirs can be neglected as a result of the screening by the free flow of charge carriers. Transport proceeds by electrons hopping between the reservoirs and the interacting region. The Landauer formula can be written as [13]

$$J = \frac{\mathrm{i}e}{2h}\int \mathrm{d}\omega \mathrm{Tr}\left[(f_L(\omega)\Gamma_L - f_R(\omega)\Gamma_R)(\mathbf{G}^r - \mathbf{G}^a) + (\Gamma_L - \Gamma_R)\mathbf{G}^<\right] \tag{4}$$

where $(\Gamma_{L/R})_{nm} = 2\pi\sum_{\alpha\in L/R}\rho_\alpha(\omega)V_{\alpha,n}(\omega)V^*_{\alpha,m}(\omega)$ are matrices coupling the interacting region to the reservoirs. $V_{\alpha,n}$ are the hopping potentials between the reservoirs and the interacting region and ρ_α is the density of states in the reservoirs. It is worth noting that the Green functions in this formula are to be calculated from the full Hamiltonian including the reservoirs, even though the reservoirs are already present in the couplings $\Gamma_{L/R}$ of the current equation.

For negligible bias voltages, knowledge of the retarded (and hence the advanced) Green functions allows the distribution Green functions to be calculated. The next step is to choose a particular Hamiltonian H and to calculate the retarded Green functions explicitly. This can be done using the equation of motion method which consists of differentiating the Green function with respect to time, thus creating higher order Green functions. In Fourier space this amounts to the following iteration rule ($\hbar = 1$):

$$\omega\langle\langle\hat{c}; c^\dagger_m\rangle\rangle = \langle\{\hat{c}, c^\dagger_m\}\rangle + \langle\langle[\hat{c}, H]; c^\dagger_m\rangle\rangle \tag{5}$$

where $\hat{c}$ can be any combination of different creation and annihilation operators and $G^r_{n,m}(\omega) = \langle\langle c_n; c^\dagger_m\rangle\rangle$ is the Fourier transform of the retarded Green function. The above equation can be applied successively to produce multiple particle Green functions. For a system of two reservoirs and N dots with n energy levels a multiple particle operator consists of a product of at most $4(nN+2)-1$ single particle operators, i.e. the creation and annihilation operators for both spin orientations in each dot level or reservoir. Therefore, it is in principle possible to obtain a closed set of equations. Clearly, it is a daunting task to calculate and solve all possible simultaneous equations, so one usually resorts to making some approximations in order to close the set of coupled equations.

3. Single dot

In order to determine a realistic, yet simple, set of approximations, consider the simple case of a single quantum dot where only one relevant level for each spin direction will be taken into account. Any lower levels are assumed to be permanently occupied and higher energy levels are always empty. The two relevant states in the dot are labelled by the electron spin quantum numbers α or $\bar{\alpha}$. A tight binding Hamiltonian will be used with a Hubbard term U describing the Coulomb interaction between the spin-up and spin-down electrons. This is analogous to the Anderson model of localized impurity states in metals [14].

$$H_1 = \sum_{k\alpha \in L,R} \epsilon_{k\alpha} c^{\dagger}_{k\alpha} c_{k\alpha} + \sum_{\alpha} \epsilon_{\alpha} c^{\dagger}_{\alpha} c_{\alpha} + U n_{\alpha} n_{\bar{\alpha}} + \sum_{k\alpha \in L,R} (V_{k\alpha} c^{\dagger}_{k\alpha} c_{\alpha} + hc) \quad (6)$$

where ϵ_{α} and $\epsilon_{k\alpha}$ are the single particle energy levels in the dot and reservoirs respectively. Transport between dot and reservoir proceeds by means of the hopping potential $V_{k\alpha}$. Any interaction that might take place with electrons in the full lower energy levels is incorporated in the definition of ϵ_{α}. The hopping potentials $V_{k\alpha}$ are taken to be real because of the time-reversal symmetry. It is required that any set of approximations yields the correct solution in the limit of zero bandwidth, i.e. negligible hopping potential. Moreover, the single particle density of states integrated over all energies must equal unity. The density of states must be non-negative at all energies. Finally, the solution should display electron–hole symmetry. It should be invariant under the transformation $\{n \to 1 - n, U \to -U, \epsilon_{\alpha} \to \epsilon_{\alpha} + U, f \to 1 - f\}$.

The crudest set of approximations (scheme 1) consistent with these conditions [15] corresponds to the Hartree approximation scheme [16] where electrons of opposite spin do not interact directly, but only through a modified average potential field. The resulting Green function is

$$\langle\langle c_{\alpha}; c^{\dagger}_{\alpha} \rangle\rangle = \frac{\omega - \epsilon_{\alpha} - U(1 - \langle n_{\bar{\alpha}} \rangle)}{(\omega - \epsilon_{\alpha})(\omega - \epsilon_{\alpha} - U) - \Sigma_{0\alpha}[\omega - \epsilon_{\alpha} - U(1 - \langle n_{\bar{\alpha}} \rangle)]} \quad (7)$$

with

$$\Sigma_{0\alpha} = \sum_{k \in L,R} \frac{|V_{k\alpha}|^2}{\omega - \epsilon_{k\alpha}} = -\mathrm{i}(\Gamma_L + \Gamma_R)/2 \quad (8)$$

where $\Gamma_{L,R} = 2\pi \rho_{L,R} |V_{L,R}|^2$. $\Sigma_{0\alpha}$ is the self-energy due to the tunnelling of the α electron and $\langle n_{\bar{\alpha}} \rangle$ is the average occupancy of the opposite spin state. The same Green function results from the method as indicated by Caroli *et al* [17], where the full Green function is calculated as a perturbation of the system without transmission to either reservoir. The occupation is the integrated product of the (diagonal) distribution function and the local density of states in the dot. Since the Green function is related to the density of states which in turn depends on the average occupation number, it means that equation (7) is to be solved self-consistently. It can be shown that the integrated density of states equals unity, subject to the condition $0 \leqslant \langle n \rangle \leqslant 1$, which is obviously satisfied in any real system.

A better approximation scheme (scheme 2) is one which neglects the simultaneous tunnelling of the electron of opposite spin, but which does not decouple the higher order Green functions as in approximation scheme 1. This yields the following Green function:

$$\langle\langle c_{\alpha}; c^{\dagger}_{\alpha} \rangle\rangle = \frac{1 - \langle n_{\bar{\alpha}} \rangle}{\omega - \epsilon_{\alpha} - \Sigma_{0\alpha}} + \frac{\langle n_{\bar{\alpha}} \rangle}{\omega - \epsilon_{\alpha} - U - \Sigma_{0\alpha}}. \quad (9)$$

As the tunnelling of the opposite spin electron is not taken into account, its creation and annihilation operators are always paired together in the higher order Green functions. The

operators for both spins do not truly intermingle, which results in the probabilistic expression for the Green function. Therefore, the same expression can be obtained by solving the Green function for the isolated site and adding an imaginary part to the site energy to include the reservoirs, i.e. the reservoirs simply serve as a source of broadening.

A more accurate method (scheme 3) only neglects terms involving correlation in the leads, valid for temperatures higher than the Kondo temperature [16]. The Green function corresponding to these approximations is [3]

$$\langle\langle c_\alpha; c_\alpha^\dagger\rangle\rangle = \frac{1-\langle n_{\bar\alpha}\rangle}{\omega-\epsilon_\alpha-\Sigma_{0\alpha}+U\Sigma_{1\alpha}(\omega-\epsilon_\alpha-U-\Sigma_{0\alpha}-\Sigma_{3\alpha})^{-1}} + \frac{\langle n_{\bar\alpha}\rangle}{\omega-\epsilon_\alpha-U-\Sigma_{0\alpha}-U\Sigma_{2\alpha}(\omega-\epsilon_\alpha-\Sigma_{0\alpha}-\Sigma_{3\alpha})^{-1}}. \tag{10}$$

The self-energies due to the tunnelling of the $\bar\alpha$ electron are defined as

$$\Sigma_{i\alpha}(\omega) = \sum_{k\in L,R} A_i^{k\bar\alpha}|V^{k\bar\alpha}|^2\left(\frac{1}{\omega-\epsilon_\alpha+\epsilon_{\bar\alpha}-\epsilon_{k\bar\alpha}}+\frac{1}{\omega-\epsilon_\alpha-\epsilon_{\bar\alpha}-U+\epsilon_{k\bar\alpha}}\right) \tag{11}$$

where $A_1^{k\bar\alpha}=f(\epsilon_{k\bar\alpha})$, $A_2^{k\bar\alpha}=1-f(\epsilon_{k\bar\alpha})$ and $A_3^{k\bar\alpha}=1$. As for scheme 2, it can be shown that the density of states integrates to unity for all values of $\langle n\rangle$.

Since the couplings to the reservoirs differ by a constant factor the distribution matrix reduces to a diagonal matrix.

$$\mathbf{F} = \frac{f_L\Gamma_L+f_R\Gamma_R}{\Gamma_L+\Gamma_R}\begin{pmatrix}1 & 0\\ 0 & 1\end{pmatrix}. \tag{12}$$

As there is only one level for each spin the current expression (4) takes an especially simple form where the current is proportional to the density of states between the Fermi levels of the reservoirs

$$J = \frac{e}{\hbar}\frac{\Gamma_L\Gamma_R}{\Gamma_L+\Gamma_R}\int \mathrm{d}\omega\rho(\omega)\left[f_L(\omega)-f_R(\omega)\right]. \tag{13}$$

The ohmic conductance is given by the integrated product of the density of states and the derivative of the Fermi function. At low temperatures the derivative of the Fermi function approximates a δ-function. A Lorentzian density of states with its broadening caused solely by tunnelling to and from the reservoirs thus gives rise to a conductance peak of height e^2/h, provided that the dot is symmetrically coupled to the reservoirs.

The three approximation schemes are compared in figures 1–3 for the case where the temperature equals the broadening due to the reservoirs. In order to distinguish between the electrons in the dot, a magnetic field is applied giving rise to a Zeeman splitting of the energy levels ($\epsilon_\alpha = 0.0U, \epsilon_{\bar\alpha}=0.1U$).

Figure 1 shows the current and the associated differential conductance through the dot when a bias voltage is applied across it, keeping the chemical potential in the right reservoir fixed ($\mu_R=-0.5U$). All three approximation schemes yield qualitatively the same results, although scheme 3 (and scheme 2 to a lesser extent) has a larger associated broadening. This is a direct consequence of the fact that scheme 3 takes the tunnelling of the oppositely charged electron into account.

In figure 2 the ohmic conductance is plotted. The approximation schemes give identical solutions for the shape and height of the major conductance peaks, but especially approximation scheme 1 gives a different result for the amplitude of the minor peaks. Moreover, an investigation of the occupation plot 3 shows that for scheme 1 the average occupation of the higher energy spin state can exceed that of the other spin state for intermediate values of the chemical potential of the reservoirs. This is clearly unphysical.

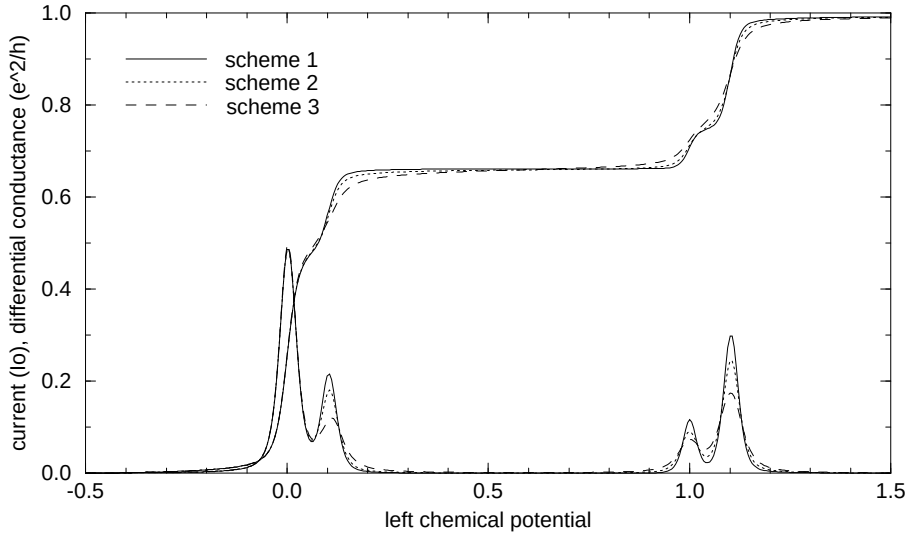

Figure 1. Current and associated differential conductance through a dot with a spin-split level for the various approximation schemes ($\mu_R = -0.5U$, $k_BT = \Gamma_L = \Gamma_R = 0.01U$, $\epsilon_\alpha = 0.0U$, $\epsilon_{\bar{\alpha}} = 0.1U$, $I_0 = 2e^2\Gamma_L\Gamma_R/\hbar(\Gamma_L + \Gamma_R)$).

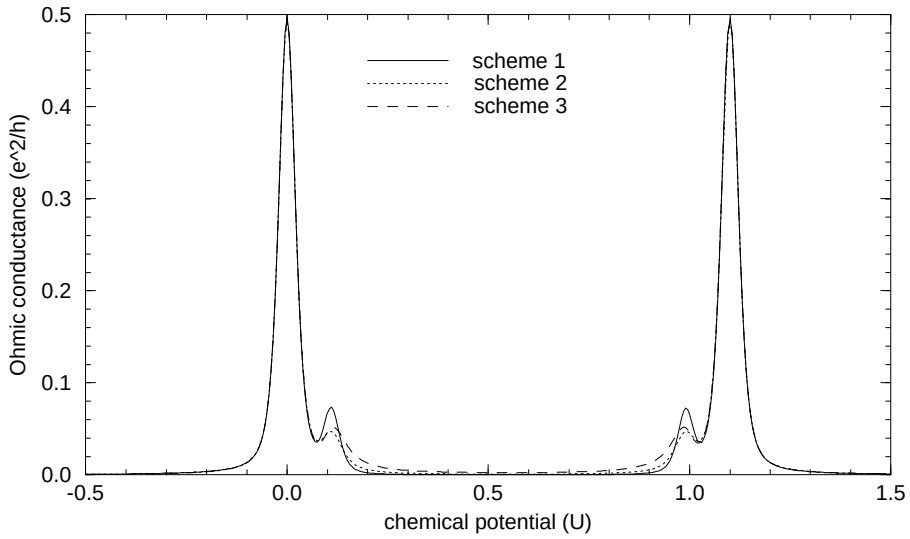

Figure 2. Ohmic conductance through a dot with a spin-split level for the various approximation schemes ($k_BT = \Gamma_L = \Gamma_R = 0.01U$, $\epsilon_\alpha = 0.0U$, $\epsilon_{\bar{\alpha}} = 0.1U$).

Both these observations justify the conclusion that scheme 1 should be dismissed as a good set of approximations.

As expected the conductance plot shows peaks at the single particle energy levels and at the same energies displaced by U. It is clear that two peaks are suppressed, which can be explained as follows. The first peak occurs when transport takes place through the lowest

level ϵ_α. As the chemical potential in the reservoirs is raised, the state ϵ_α will start to fill up. When the chemical potential lines up with $\epsilon_{\tilde{\alpha}}$, level ϵ_α will be mostly occupied (see figure 3) thus putting the Coulomb blockade in place and impeding the flow of electrons through level $\epsilon_{\tilde{\alpha}}$. This results in a highly suppressed conductance peak. Because of the electron–hole symmetry a similar situation occurs at much higher values of the chemical potential.

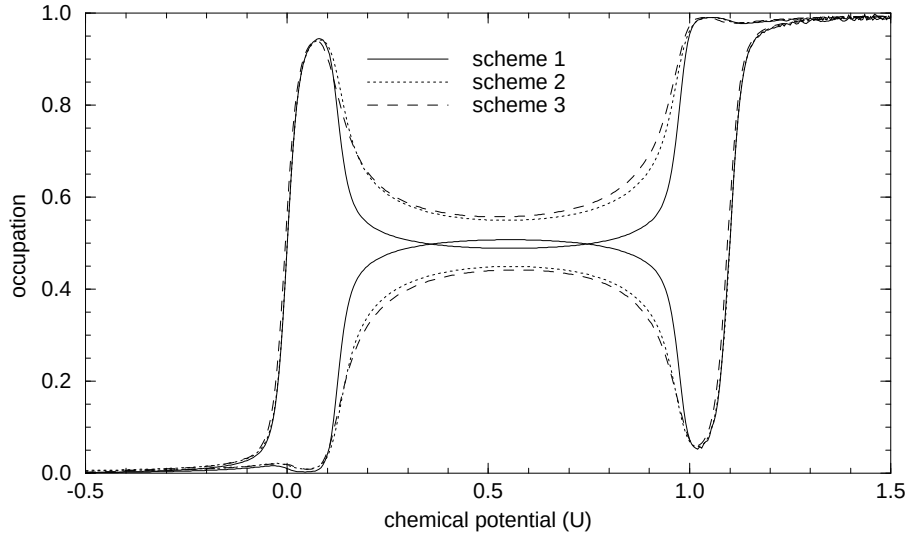

Figure 3. Occupation of a dot with a spin-split level for the various approximation schemes ($k_BT = \Gamma_L = \Gamma_R = 0.01U$, $\epsilon_\alpha = 0.0U$, $\epsilon_{\tilde{\alpha}} = 0.1U$). The two sets of curves refer to the occupation of the α and $\tilde{\alpha}$ states.

Approximation schemes 2 and 3 seem to give results which are closely in accordance with each other. The main difference is that approximation scheme 3 produces a larger associated broadening. Although slightly better, scheme 3 is harder to manipulate numerically, whereas scheme 2 is much more stable. Therefore approximation scheme 2 will be employed here.

4. Two dots

4.1. Formalism

The single dot Hamiltonian can easily be extended to describe two quantum dots in series. As before, assume that there is only one spin-split level per dot and that the electrons experience an on-site interaction energy $U_{1/2}$.

$$\begin{aligned} H_2 = & \sum_{k\alpha\in L,R} \epsilon_{k\alpha} c^\dagger_{k\alpha} c_{k\alpha} + \sum_\alpha (\epsilon_{1\alpha} c^\dagger_{1\alpha} c_{1\alpha} + \epsilon_{2\alpha} c^\dagger_{2\alpha} c_{2\alpha}) \\ & + U_1 n_{1\alpha} n_{\bar{1}\alpha} + U_2 n_{2\alpha} n_{\bar{2}\alpha} + \sum_\alpha V_M (c^\dagger_{1\alpha} c_{2\alpha} + hc) \\ & + \sum_{k\alpha\in L} (V_{k\alpha} c^\dagger_{k\alpha} c_{1\alpha} + hc) + \sum_{k\alpha\in R} (V_{k\alpha} c^\dagger_{k\alpha} c_{2\alpha} + hc). \end{aligned} \tag{14}$$

As before the dots are coupled to the reservoirs by the hopping potentials $V_{k\alpha}$, but there is also some coupling V_M between the dots. In this representation the coupling matrices for each spin are given by

$$\Gamma_L = \begin{pmatrix} \Gamma_L & 0 \\ 0 & 0 \end{pmatrix} \qquad \Gamma_R = \begin{pmatrix} 0 & 0 \\ 0 & \Gamma_R \end{pmatrix}. \tag{15}$$

Now that there is more than one dot in the interacting region, it is clear that the correlations between the occupation numbers of the dots become important, since the occupation of one dot will depend on the occupation of the other. The equivalent of approximation scheme 1 actually ignores this correlation. Here the approximation scheme 2 will be employed, where the reservoirs are included in the form of a self-energy. The single particle Green function matrix for spin α is given by

$$\begin{aligned} \mathbf{G}^r = {} & \frac{\langle n_{1\bar{\alpha}} n_{2\bar{\alpha}} \rangle}{(\omega - \epsilon'_{1\alpha} - U_1)(\omega - \epsilon'_{2\alpha} - U_2) - V_M^2} \begin{pmatrix} \omega - \epsilon'_{2\alpha} - U_2 & V_M \\ V_M & \omega - \epsilon'_{1\alpha} - U_1 \end{pmatrix} \\ & + \frac{\langle n_{1\bar{\alpha}}(1 - n_{2\bar{\alpha}}) \rangle}{(\omega - \epsilon'_{1\alpha} - U_1)(\omega - \epsilon'_{2\alpha}) - V_M^2} \begin{pmatrix} \omega - \epsilon'_{2\alpha} & V_M \\ V_M & \omega - \epsilon'_{1\alpha} - U_1 \end{pmatrix} \\ & + \frac{\langle n_{2\bar{\alpha}}(1 - n_{1\bar{\alpha}}) \rangle}{(\omega - \epsilon'_{1\alpha})(\omega - \epsilon'_{2\alpha} - U_2) - V_M^2} \begin{pmatrix} \omega - \epsilon'_{2\alpha} - U_2 & V_M \\ V_M & \omega - \epsilon'_{1\alpha} \end{pmatrix} \\ & + \frac{\langle (1 - n_{1\bar{\alpha}})(1 - n_{2\bar{\alpha}}) \rangle}{(\omega - \epsilon'_{1\alpha})(\omega - \epsilon'_{2\alpha}) - V_M^2} \begin{pmatrix} \omega - \epsilon'_{2\alpha} & V_M \\ V_M & \omega - \epsilon'_{1\alpha} \end{pmatrix} \end{aligned} \tag{16}$$

where $\epsilon'_{1\alpha} = \epsilon_{1\alpha} - \frac{i}{2}\Gamma_L$, $\epsilon'_{2\alpha} = \epsilon_{2\alpha} - \frac{i}{2}\Gamma_R$. As for the single dot case, the Green functions have a straightforward probabilistic interpretation. They treat the electrons of opposite spin $\bar{\alpha}$ as static entities whose main influence is to change the effective site energy of the electrons of spin α by U. Each Green function is simply a sum over effective *non-interacting* Green functions each weighted by the probability of a particular realization of the occupation numbers for the opposite spin states. Of course the single particle energy levels have to be adjusted to correspond to the correct occupations of the opposite spin states.

This form of the Green function has some important consequences.

- First of all the distribution, retarded and advanced self-energies can be written in terms of the coupling matrices: $\Sigma^< = i(f_L\Gamma_L + f_R\Gamma_R)$ and $\Sigma^r - \Sigma^a = -i(\Gamma_L + \Gamma_R)$. Substitution of the equalities $\mathbf{G}^< = \mathbf{G}^r\Sigma^<\mathbf{G}^a$ and $\mathbf{G}^r - \mathbf{G}^a = \mathbf{G}^r(\Sigma^r - \Sigma^a)\mathbf{G}^a$ into equation (4) yields a condensed form of the current formula for non-interacting systems.

$$J = \frac{e}{h}\int \mathrm{d}\omega [f_L(\omega) - f_R(\omega)] \mathrm{Tr}\left[\Gamma_L \mathbf{G}^a \Gamma_R \mathbf{G}^r\right]. \tag{17}$$

  Using equations (15) for the double dot this reduces to

$$J = \frac{e}{h}\sum_\alpha \int \mathrm{d}\omega [f_L(\omega) - f_R(\omega)] \Gamma_L \Gamma_R G^a_{12} G^r_{21}. \tag{18}$$

- Secondly, the coupling matrices are no longer proportional, which results in a non-diagonal form of the distribution matrix at finite bias.

$$\mathbf{F} = \mathbf{G}^r \begin{pmatrix} f_L & 0 \\ 0 & f_R \end{pmatrix} (\mathbf{G}^r)^{-1}. \tag{19}$$

- Thirdly, the probabilistic form of the Green functions warrants a statistical approach for the multiplication of Green functions. Since the Green functions are probabilistic sums over non-interacting Green functions, products of Green functions must be expressed as probabilistic sums over the products of the appropriate non-interacting Green functions.

- Fourthly, higher order Green functions, needed to calculate correlations of the type $\langle n_{1\alpha} n_{2\alpha} \rangle$, can also be reduced to a sum over non-interacting Green functions. For a non-interacting system it can be shown that

$$\langle n_1 n_2 \rangle = \langle n_1 \rangle \langle n_2 \rangle - \langle c_1^\dagger c_2 \rangle \langle c_2^\dagger c_1 \rangle. \tag{20}$$

  In the presence of interaction on the dots, the correlation $\langle n_{1\alpha} n_{2\alpha} \rangle$ is obtained by taking the probabilistic sum over all possible occupation realizations of the opposite spin states.

Taking the four points above into account, the current and conductance characteristics can be calculated.

4.2. Simple two-level dots

Figure 4 shows the ohmic conductance through two dots which are identical in all respects apart from a relative energy off-set of $0.4U$. In order to be able to interpret the conductance plots more easily the average occupation numbers for the four single-particle states are also plotted.

In the limit of negligible coupling between the dots, the occupation for each dot is determined solely by the coupling to the adjoining reservoir. This is identical to the single dot case (cf figure 3). The ohmic conductance displays peaks at all the single particle energy levels and at the same energies displaced by U. Similar to the conductance through a single dot (see figure 2), the peaks come in pairs separated by the Zeeman energy $\epsilon_{\bar{\alpha}} - \epsilon_\alpha$. As it has been explained for the single dot, one of the peaks of each pair is suppressed as a result of the Coulomb blockade in the dot. However, it is apparent from figure 4(a) that there is also a modulation of the height of pairs of peaks. For instance the first major peak is noticeably larger than the second peak. The current path that gives rise to the first major peak encompasses the levels $\epsilon_{1\alpha}$ and $\epsilon_{2\alpha}$. At the chemical potential at which the second major peak occurs, the first dot will be virtually completely occupied and the Coulomb blockade will be in place. Therefore the dominant contribution to the current will come from the energy levels $\epsilon_{1\alpha} + U$ and $\epsilon_{2\alpha}$. In the case of figure 4(a) the dominant levels for the second peak are energetically further apart than those for the first peak, which explains why the second pair of peaks is slightly suppressed. In short, the form of the conductance plot for negligible inter-dot coupling V_M can be understood by realizing that electrons contribute to the transport only when the Coulomb barrier is overcome in both the first and the second dot.

As the coupling between the dots is increased, the energy levels in the dots start to interact, repelling one another. The conductance peaks are shifted in energy. When the coupling between the dots becomes appreciable compared to the energy level difference $\epsilon_{2\alpha} - \epsilon_{1\alpha}$ for the decoupled dots, the number of peaks in the conductance can increase to a number that is greater than the total number of single particle energy levels. This is a result of the fact that the amount by which a level is repelled depends on the energy difference with the level by which it is repelled. For instance, an original level at an energy $\epsilon_{1\alpha}$ can be repelled to two different resultant energies depending on whether it interacts with level $\epsilon_{2\alpha}$ or $\epsilon_{2\alpha} + U$. This causes a conductance peak both to shift in energy and to split. This is particularly significant when a level is repelled into opposite directions by the two possible levels it could interact with. This happens at intermediate values of the chemical potential, and this explains why splitting can start to be observed for the middle peak pairs of figure 4(c) but not for the peaks at more extreme values of the chemical potential.

In figure 5 the current through the two dots is plotted as a function of the chemical potential in the left reservoir, keeping the chemical potential in the right reservoir fixed.

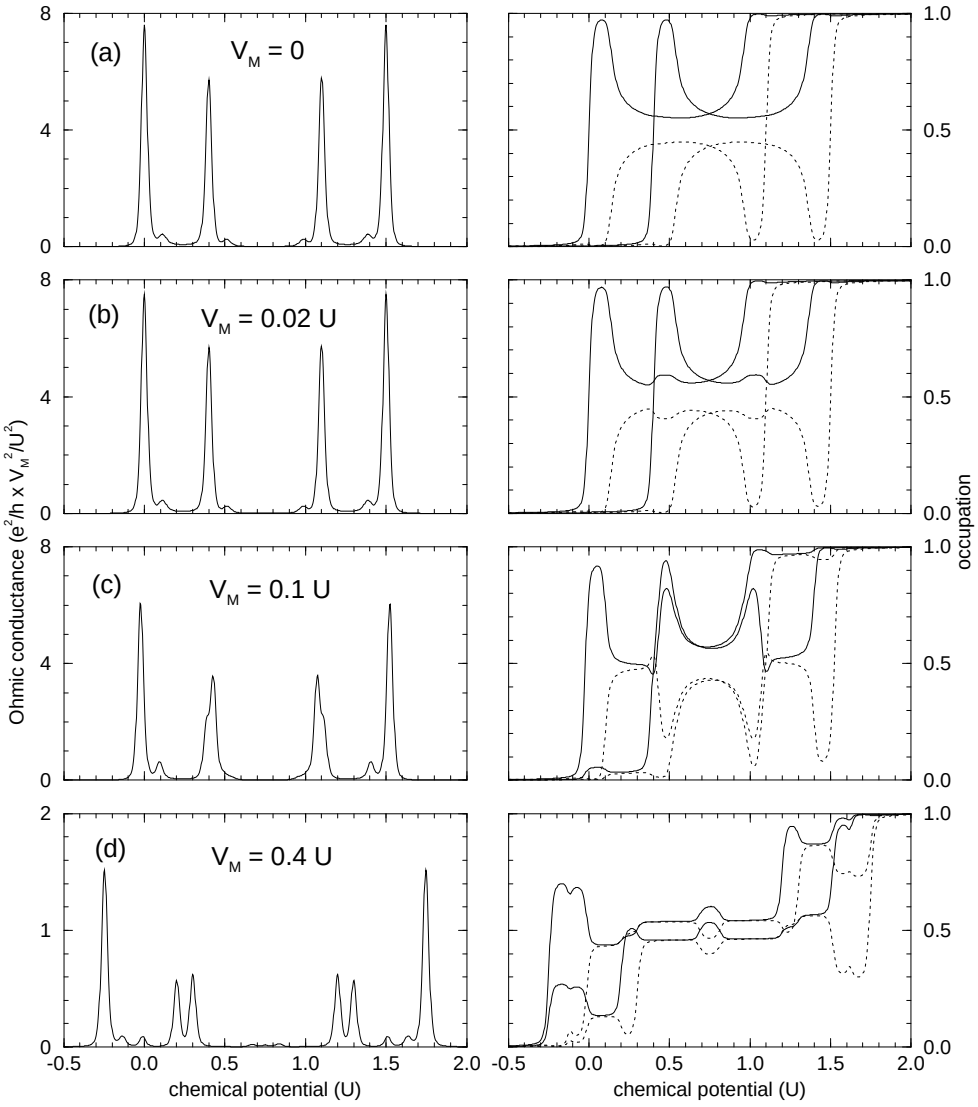

Figure 4. Ohmic conductance through two dots each with a level for both spins, using various coupling constants V_M ($U_1 = U_2 = U$, $k_BT = \Gamma_L = \Gamma_R = 0.01U$, $\epsilon_{1\alpha} = 0.0U$, $\epsilon_{1\bar{\alpha}} = 0.1U$, $\epsilon_{2\alpha} = 0.4U$, $\epsilon_{2\bar{\alpha}} = 0.5U$). In the occupation plots the solid lines correspond to the states of spin α, the dotted lines to the states of spin $\bar{\alpha}$.

The I–V characteristics are studied as the coupling between the dots is increased.

In the limit of negligible coupling the occupation of each dot is completely determined by the tunnelling of electrons to and from the adjoining reservoir. The barrier between the dots is clearly the current limiting segment, so that the current is proportional to V_M^2 (see figure 5(a)). Transport can proceed because the wavefunctions corresponding to the levels in the first dot can leak slightly into the second dot and vice versa, thus creating current paths. This explains why there is a marked increase in the current at $\mu_L = \epsilon_{1\alpha}$, $\mu_L = \epsilon_{2\alpha}$ and $\mu_L = \epsilon_{2\bar{\alpha}}$. Note that no current step occurs at $\mu_L = \epsilon_{1\bar{\alpha}}$, even though an extra current path

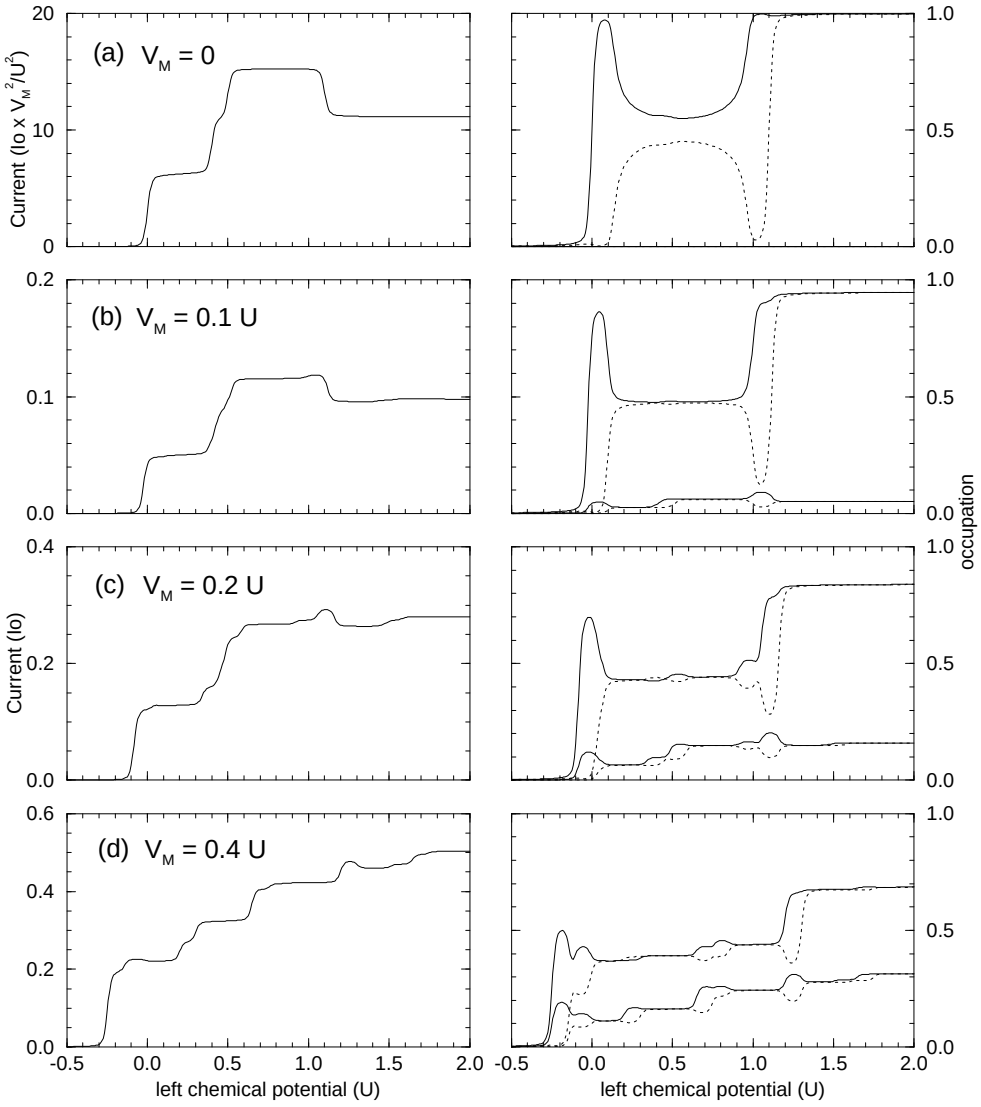

Figure 5. Current through two dots each with a level for both spins, using various coupling constants V_M ($\mu_R = -2.0U$, $U_1 = U_2 = U$, $k_BT = \Gamma_L = \Gamma_R = 0.01U$, $\epsilon_{1\alpha} = 0.0U$, $\epsilon_{1\bar{\alpha}} = 0.1U$, $\epsilon_{2\alpha} = 0.4U$, $\epsilon_{2\bar{\alpha}} = 0.5U$). In the occupation plots the solid lines correspond to the states of spin α, the dotted lines to the states of spin $\bar{\alpha}$.

becomes available. This is most easily comprehended by drawing a distinction between the number of current paths and the number of effective current paths. A current path consists of a composite state which is a mixture of a state in the first dot and one in the second dot. A current path can be said to be effective when it can be used constantly. For example, it is true that a second current path becomes available at $\mu_L = \epsilon_{1\bar{\alpha}}$. However, the number of effective paths remains fixed at 1, since the Coulomb blockade in the first dot prevents the paths from being used simultaneously.

The most notable feature of figure 5(a) is the region of negative differential conductance

around $\mu_L = \epsilon_{1\alpha} + U$. This is the energy at which the single particle levels in the first dot are both likely to be occupied. The dominant current contribution arises from the interaction of the levels $\epsilon_1 + U$ with the levels ϵ_2. As these states are energetically further separated than the levels ϵ_1 and ϵ_2, this means that there is less overlap of the wavefunctions in the two dots which accounts for the drop in current.

4.3. Multi-level dots

Finally, the more realistic case of the ohmic conductance through a double dot with an infinite number of energy levels will be calculated. The simple case of negligible broadening and small inter-dot coupling will be considered. The coupling to the reservoirs in the 'site' representation is given by the following matrices:

$$\Gamma_L = \begin{pmatrix} \hat{\Gamma}_L & \vdots & \hat{0} \\ \cdots & \ddots & \cdots \\ \hat{0} & \vdots & \hat{0} \end{pmatrix} \qquad \Gamma_R = \begin{pmatrix} \hat{0} & \vdots & \hat{0} \\ \cdots & \ddots & \cdots \\ \hat{0} & \vdots & \hat{\Gamma}_R \end{pmatrix}. \tag{21}$$

The matrix is subdivided into four infinite sub-matrices, corresponding to coupling either between levels of the same dot or between levels of different dots, e.g., the top left sub-matrix includes all couplings between levels of the first dot. The sub-matrices $\hat{\Gamma}_{L/R}$ are defined as a matrices whose elements are all given by $\Gamma_{L/R}$. As before the current will be determined using equation (17). Substitution of the coupling matrices, and taking the limit of an infinitesimal (ohmic) bias across the system yields the conductance equation

$$G = \frac{e^2}{h} \int \mathrm{d}\omega \frac{\Gamma_L \Gamma_R}{4k_B T \cosh^2(\frac{\omega-\mu}{2k_B T})} \left| \sum_{i\in\mathrm{dot1}} \sum_{j\in\mathrm{dot2}} G^r_{ij}(\omega) \right|^2. \tag{22}$$

Analogous to expression (18) the conductance only depends on the Green functions between states in different dots. Treating the inter-dot coupling V_M as a small perturbation allows these off-diagonal Green functions to be written as $G^r_{ij}(\omega) = G^r_i(\omega) V_M G^r_j(\omega)$ so that

$$G = \frac{e^2}{h} \int \mathrm{d}\omega \frac{\Gamma_L \Gamma_R V_M^2}{4k_B T \cosh^2(\frac{\omega-\mu}{2k_B T})} \left| \sum_{i\in\mathrm{dot1}} G^r_i(\omega) \right|^2 \left| \sum_{j\in\mathrm{dot2}} G^r_j(\omega) \right|^2. \tag{23}$$

In this approximation the diagonal elements $G^r_i(\omega)$ of the Green function are identical to those of the single dot with multiple levels [3]. Hence

$$\Gamma_L \left| \sum_{i\in\mathrm{dot1}} G^r_i(\omega) \right|^2 = \Gamma_L \left| \sum_{i\in\mathrm{dot1}} \sum_{N_1} \frac{P_i(N_1)}{\omega - \epsilon_i + i\Gamma_L/2 - N_1 U_1} \right|^2 \tag{24}$$

where $P_i(N_1)$ is the probability that the first dot contains N_1 electrons on levels other than ϵ_i. In the limit of negligible broadening this becomes

$$\begin{aligned} \Gamma_L \left| \sum_{i\in\mathrm{dot1}} G^r_i(\omega) \right|^2 &= 2\pi \sum_{i\in\mathrm{dot1}} \sum_{N_1} P_i(N_1) \delta(\omega - \epsilon_i - N_1 U_1) \\ &\quad + \Gamma_L \left(\sum_{i\in\mathrm{dot1}} \sum_{N_1} \frac{P_i(N_1)}{\omega - \epsilon_i - N_1 U_1} \right)^2. \end{aligned} \tag{25}$$

The first part of the expression shows the behaviour at energies coinciding with an energy level whereas the second part gives the off-resonance contribution. A similar expression

may be obtained for the Green functions of the second dot. Note that the limit of small broadening excludes the possibility of energy levels in the two dots matching up exactly (this case will be examined later in more detail), so that the conductance formula 23 can be rewritten as

$$G = \frac{e^2}{h}\int \mathrm{d}\omega \frac{2\pi V_M^2}{4k_B T \cosh^2(\frac{\omega-\mu}{2k_B T})} \times \left[\sum_{i\in\mathrm{dot1}}\sum_{N_1}\Gamma_R P_i(N_1)\delta(\omega-\epsilon_i-N_1U_1)\left(\sum_{j\in\mathrm{dot2}}\sum_{N_2}\frac{P_j(N_2)}{\omega-\epsilon_j-N_2U_2}\right)^2 + \sum_{j\in\mathrm{dot2}}\sum_{N_2}\Gamma_L P_j(N_2)\delta(\omega-\epsilon_j-N_2U_2)\left(\sum_{i\in\mathrm{dot1}}\sum_{N_1}\frac{P_i(N_1)}{\omega-\epsilon_i-N_1U_1}\right)^2\right]. \quad (26)$$

In figure 6 the ohmic conductance has been plotted for a system where the dots have a different level spacing and Coulomb interaction. As expected at low temperatures, the conductance peaks are largest at values of the chemical potential where the charge degeneracy points of the two dots are close in energy. At the charge degeneracy point between the occupations N and $N+1$ the $(N+1)$th single particle level is dominant. As the temperature is raised there is a higher probability of other levels contributing to the current. This has a particularly strong effect when any of the newly available subsidiary levels very nearly match up (as at $\mu \simeq -4.7U$). Otherwise a rise in temperature simply causes the peaks to be smeared. At higher temperatures the periodicity of the smaller dot $U_2 + \Delta_{\epsilon_2}$ can easily be estimated from the spacing of the peaks in the conductance plot.

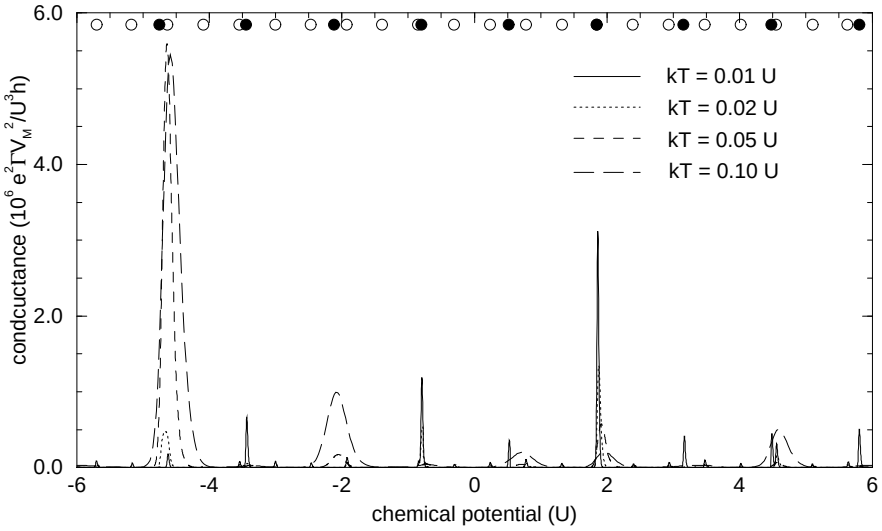

Figure 6. Ohmic conductance through two dots with multiple levels in the limit of small coupling Γ, V_M ($U_1 = 0.41U$, $U_2 = U$, $\Delta_{e_1} = 0.13U$, $\Delta_{e_2} = 0.32U$, $\Gamma_L = \Gamma_R = \Gamma$). The open and full circles indicate the positions at which the average occupation increases by one for dot 1 and 2 respectively.

At this stage it is useful to analyse the height and shape of the conductance peaks in more detail. Moreover, in order to compare the coherent case with other tunnelling mechanisms, it would be helpful to obtain an expression for the current through the double

dot at finite bias as a function of the gate potential of one of the dots. At low temperatures these quantities can be investigated by just considering the dominant levels in each of the dots. Their energy difference is simply the separation Δ between the nearest charge degeneracy points. Since this is now a non-interacting system, the Green functions G_{12} of the current formula (18) can be calculated exactly. It is also possible to include the effect of non-negligible dot-reservoir and inter-dot coupling. This yields

$$J = \frac{e}{h}\int \mathrm{d}\omega \frac{\Gamma_L\Gamma_R V_M^2 (f_L - f_R)}{\left[\omega^2 - (\Delta^2 + 4V_M^2 + \Gamma_L\Gamma_R)/4\right]^2 + \frac{1}{4}\left[\omega(\Gamma_L + \Gamma_R) + \frac{\Delta}{2}(\Gamma_L - \Gamma_R)\right]^2}. \tag{27}$$

First, consider the peak characteristics of the ohmic conductance. This is obtained simply by differentiating with respect to μ_L and setting $\mu_L = \mu_R = \mu$. Thus, for $\Gamma_L = \Gamma_R = \Gamma$, one obtains

$$G = \frac{e^2}{h}\int \mathrm{d}\omega \frac{1}{4k_BT\cosh^2\left(\frac{\omega-\mu}{2k_BT}\right)} \frac{16\Gamma^2 V_M^2}{\left[4\omega^2 - \Delta^2 - 4V_M^2 + \Gamma^2\right]^2 + 4\Gamma^2(\Delta^2 + 4V_M^2)}. \tag{28}$$

This shows that the conductance is determined by the product of a thermal broadening factor and a term which is a Lorentzian in ω^2 of width $\Gamma\Lambda$ where $\Lambda = \sqrt{\Delta^2 + 4V_M^2}$. Depending on the relative width of the two terms, two limiting cases will be of relevance.

In the limiting case of small reservoir-dot coupling $k_BT \gg \sqrt{\Lambda\Gamma}$ the conductance can be rewritten as

$$G = \frac{e^2}{h}\frac{\Gamma V_M^2}{2k_BT(\Delta^2 + 4V_M^2 + \Gamma^2)} \begin{cases} \cosh^{-2}\left(\frac{\mu}{2k_BT}\right) & \text{if } \Gamma \geqslant \Lambda \\ \sum_{\pm}\frac{1}{2}\cosh^{-2}\left(\frac{\mu \pm \frac{1}{2}\sqrt{\Delta^2+4V_M^2-\Gamma^2}}{2k_BT}\right) & \text{if } \Gamma < \Lambda \end{cases} \tag{29}$$

which is clearly consistent with expression 26 for negligible reservoir-dot and inter-dot coupling. This shows that, as a result of the level repulsion and the broadening, the conductance does in fact not diverge at $\Delta = 0$ in this limit. Moreover, the peak height is inversely proportional to the temperature, as was the case for the ohmic conductance through a single dot.

The question whether the conductance diverges at all will now be considered by taking the opposite limit of vanishing temperature $k_BT \ll \sqrt{\Lambda\Gamma}$. It appears that the conductance either has a single peak or a split peak.

$$G_{\max} = \frac{e^2}{h} \begin{cases} \dfrac{16\Gamma^2 V_M^2}{(\Delta^2 + 4V_M^2 + \Gamma^2)^2} & \text{at } \mu = 0 \qquad \text{if } \Gamma \geqslant \Lambda \\ \dfrac{4V_M^2}{\Delta^2 + 4V_M^2} & \text{at } \mu = \pm\frac{1}{2}\sqrt{\Delta^2 + 4V_M^2 - \Gamma^2} \qquad \text{if } \Gamma < \Lambda \end{cases} \tag{30}$$

This shows that the conductance will not diverge but has a maximum value imposed by the conductance quantum e^2/h, which can only be reached when $\Delta = 0, \Gamma_L = \Gamma_R = \Gamma$ and $V_M \geqslant \Gamma/2$. For asymmetric tunnelling barriers to the reservoirs, the conductance is maximized at $V_M = \frac{1}{2}\sqrt{\Gamma_L^2 + \Gamma_R^2}$ and gives a maximum conductance of $(e^2/h)8\Gamma_L\Gamma_R(\Gamma_L^2 + \Gamma_R^2)/(\Gamma_L + \Gamma_R)^4$.

Secondly, an expression will be derived describing the current peaks which occur at finite bias when the gate voltage of one of the dots is raised. As before, only a single level per dot will be taken into account. Assuming that the energy window $\mu_L - \mu_R$ is

sufficiently large, the integral in the current equation 27 can be solved analytically by finding the residues of the poles of the integrand in the Argand plane. This yields

$$J_{\text{peak}} = \frac{e}{h} \frac{V_M^2(\Gamma_L + \Gamma_R)}{\Delta^2 + (\Gamma_L + \Gamma_R)^2/4 + V_M^2(\Gamma_L + \Gamma_R)^2/\Gamma_L\Gamma_R} \tag{31}$$

The current peak has a Lorentzian line shape with a width that is at least as large as the combined width of the single particle levels in the two dots. This is consistent with the experimentally observed line shape [18]. In the limit of large coupling the same maximum current results as for the single dot case.

5. Summary

In conclusion, a coherent system of one or more weakly coupled quantum dots with Coulomb interaction can be well described using Green functions of a probabilistic nature. In a double dot, the modes of the individual dots are coupled together. The resulting level repulsion can lead to a complex form of the ohmic conductance and the current. Regions of negative differential conductance are likely to occur. The ohmic conductance through two dots with multiple levels is dominated by the matching energy levels.

The maximum conductance through a double dot e^2/h is reached at low temperatures in the symmetric case of aligned levels $\Delta = 0$, identical coupling to the reservoirs $\Gamma_L = \Gamma_R = \Gamma$ and $V_M \geqslant \Gamma/2$.

The peaks that occur in the current as the gate potential of one of the dots is varied while keeping the voltage bias across the dots fixed have a Lorentzian line shape with a width at least as large as the combined broadening of the individual dot levels.

References

[1] Reed M A, Randall J N, Aggarwal R J, Matyi R J, Moore T M and Wetsel A E 1988 *Phys. Rev. Lett.* **60** 535
[2] Beenakker C W J 1991 *Phys. Rev.* B **44** 1646
[3] Meir Y, Wingreen N S and Lee P A 1991 *Phys. Rev. Lett.* **66** 3048
[4] Amman M, Wilkins R, Ben-Jacob E, Maker P D and Jaklevic R C 1991 *Phys. Rev.* B **43** 1146
[5] Ruzin I M, Chandrasekhar V, Levin E I and Glazman L I 1992 *Phys. Rev.* B **45** 13469
[6] Kemerink M and Molenkamp L W 1994 *Appl. Phys. Lett.* **65** 1012
[7] Payne M C1986 *J. Phys. C: Solid State Phys.* **19** 1145
[8] Weil T and Vinter B1987 *Appl. Phys. Lett.* **50** 1281
[9] Yacoby A, Heiblum M, Mahalu D and Shtrikman H 1995 *Phys. Rev. Lett.* **74** 4047
[10] Keldysh L V1965 *Sov. Phys.–JETP* **20** 1018
[11] Rammer J 1986 *Rev. Mod. Phys.* **58** 323
[12] Landauer R 1970 *Philos. Mag.* **21** 863
[13] Meir Y and Wingreen N S 1992 *Phys. Rev. Lett.* **68** 2512
[14] Anderson P W 1961 *Phys. Rev.* **124** 41
[15] Hubbard J 1963 *Proc. R. Soc.* A **276** 238
[16] Lacroix C 1981 *J. Phys. F: Met. Phys* **11** 2389
[17] Caroli C, Combescot R, Nozieres P and Saint-James D 1971 *J. Phys. C: Solid State Phys.* **4** 916
[18] van der Vaart N C, Godijn S F, Nazarov Y V, Harmans C J P M and Mooij J E 1995 *Phys. Rev.* **74** 4702